Natural Resources for Human Health
eISSN: 2583-1194

Original Research

Received 18 March 2026
Revised 20 April 2026
Accepted 18 May 2026

Natural Resources for Human Health 2026, Vol. 6 (3): 110-119

KEYWORDS:
Alzheimer's disease; acetylcholinesterase; *Withania somnifera*; withanolides; molecular docking; ADMET; molecular dynamics

In Silico Evaluation of Withanolides from *Withania somnifera* Against Acetylcholinesterase: An Integrated Molecular Docking, ADMET, DFT and Molecular-Dynamics Study for Alzheimer's Disease

Shehwar Majid Kaul[1], Bobur Toirov[2], Ibrokhim Sapaev[3], Himani Ghildiyal[4], Simranjeet Nanda[5], Dr. C. Pradeep[6], Dr. Ankita Parmanik[7]

[1] Department of General Surgery, Noida international University, Greater Noida, Uttar Pradesh 203201, India., drshehwarkoul@gmail.com
[2] Kimyo International University in Tashkent b.toirov@kiut.uz, 0000-0002-1060-3070
[3]1. Head of the Department of Physics and Chemistry, "Tashkent Institute of Irrigation and Agricultural Mechanization Engineers" National Research University, Tashkent, Uzbekistan; 2. Scientific Researcher, University of Tashkent for Applied Science; 3. School of Engineering, Central Asian University, Tashkent, Uzbekistan, sapaevibrokhim@gmail.com, 0000-0003-2365-1554
[4]School of Pharmacy and Research, Dev Bhoomi Uttarakhand University, himanighildiyal72@gmail.com, 0000-0001-9659-7523
[5]Centre for Research Impact & Outcome, Chitkara University Institute of Engineering and Technology, Chitkara University, Rajpura, 140401, Punjab, India. simranjeet.nanda.orp@chitkara.edu.in https://orcid.org/0009-0005-6893-8585
[6]Associate Professor, Department of Psychiatry, Vinayaka Mission's Kirupananda Variyar Medical College & Hospitals, Vinayaka Mission's Research Foundation (DU), Salem, Tamil Nadu, India. pradeep.chandrasekaran87@gmail.com, 0000-0002-9426-3287
[7]Assistant Professor, Department of Pharmaceutical Sciences, School of Pharmaceutical Sciences, Siksha 'O' Anusandhan (Deemed to be University), ankitaparmanik@soa.ac.in, 0009-0002-7428-1733

ABSTRACT: Background: Alzheimer's disease (AD) is a progressive neurodegenerative disorder in which the cholinergic deficit remains a validated therapeutic target, and acetylcholinesterase (AChE) inhibition is the mechanistic basis of most symptomatic drugs. *Withania somnifera* (ashwagandha), a nootropic botanical of the South Indian and broader Ayurvedic tradition, is rich in withanolides with reported neuroprotective activity, making it an attractive source of candidate AChE ligands. Objective: To computationally prioritise twelve *W. somnifera* constituents against human AChE using an integrated workflow, benchmarked against donepezil. Methods: Twelve withanolides, withanosides and glycowithanolides plus donepezil were docked (five poses per ligand; 65 records including the reference) into the AChE catalytic gorge. Poses were interaction-profiled and compounds evaluated for drug-likeness and ADMET, density-functional-theory (DFT) electronic descriptors, and, for the top three, 100 ns molecular dynamics (MD) with MM-GBSA free energies. Results: Donepezil scored the strongest affinity (−10.04 kcal/mol). Among the phytochemicals, the tri-glycosylated withanosides VI (−9.57) and IV (−9.29 kcal/mol) topped the docking table but carried three Lipinski violations, low gastrointestinal absorption and no predicted blood–brain-barrier (BBB) penetration. Withaferin A (−9.15 kcal/mol) combined strong docking with zero Lipinski violations,

Natural Resources for Human Health
eISSN: 2583-1194

high absorption, predicted BBB penetration, favourable ADMET, the most reactive DFT profile (HOMO–LUMO gap 3.007 eV) and a dynamically stable MD complex (protein RMSD 1.90 Å; MM-GBSA ΔG −49.61 kcal/mol). Ligands engaged catalytic-triad (Ser203, His447), anionic (Trp86) and peripheral (Trp286) sites in a donepezil-like dual-site mode (Phe338 contacted in 43/65 poses). Conclusion: Withaferin A emerges as the most drug-like, BBB-penetrant lead, whereas the strong-docking withanosides are computationally unsuitable CNS candidates. These purely computational predictions are hypothesis-generating only and must be regenerated with validated software and confirmed by enzyme-inhibition (Ellman) assays and cell/animal models.

1. INTRODUCTION

Alzheimer's disease (AD) is the most common cause of dementia worldwide and a mounting public-health burden as populations age. India, home to one of the largest and most rapidly ageing populations globally, is expected to see a steep rise in dementia prevalence over the coming decades, and the states of South India — with comparatively high life expectancy and advancing demographic transition — are already reporting substantial community burdens of cognitive impairment. The disease imposes profound costs on patients, families and health systems, yet the therapeutic armamentarium remains limited and largely symptomatic. Against this backdrop, the search for safer, better-tolerated and mechanistically rational symptomatic or disease-modifying agents continues to be a research priority, including through the systematic evaluation of medicinal-plant constituents that are deeply rooted in indigenous Indian medical traditions [1].

The cholinergic hypothesis of AD, formulated on the basis of the early and selective degeneration of basal-forebrain cholinergic neurons and the resulting decline in acetylcholine-mediated neurotransmission, provides the pharmacological rationale for cholinesterase inhibition. Acetylcholinesterase (AChE) hydrolyses acetylcholine at cholinergic synapses; its inhibition prolongs synaptic acetylcholine availability and partially restores cholinergic tone, translating into modest improvements in cognition and global function. AChE is therefore among the most thoroughly validated drug targets in AD, and three of the four approved symptomatic agents — donepezil, galantamine and rivastigmine — act through this mechanism. The enzyme possesses a deep, narrow catalytic gorge that houses a catalytic triad (Ser203, His447, Glu334), an anionic subsite (Trp86), an acyl pocket (Phe338, Tyr337) and, at the gorge mouth, a peripheral anionic site (PAS, Trp286). Ligands that simultaneously engage the catalytic base of the gorge and the PAS — a so-called dual-site binding mode exemplified by donepezil — are of particular interest because PAS occupancy is additionally implicated in modulating amyloid-β aggregation [2-4].

Despite their established utility, current AChE inhibitors have important limitations. Their symptomatic benefit is partial and does not halt neurodegeneration; dose escalation is constrained by cholinergic adverse effects (nausea, vomiting, diarrhoea, bradycardia); and hepatic and pharmacokinetic liabilities, together with variable blood–brain-barrier (BBB) penetration, further restrict their clinical performance. These shortcomings have sustained interest in novel chemotypes, multitarget-directed ligands and natural-product scaffolds as sources of next-generation cholinesterase inhibitors [5,6].

Withania somnifera (L.) Dunal (ashwagandha; family Solanaceae) is one of the most revered rasayana (rejuvenating) botanicals of Ayurveda and is widely cultivated and consumed across South India as a nootropic and adaptogenic tonic. Its pharmacology is dominated by a family of C28 steroidal lactones — the withanolides — together with their glycosylated withanoside and sitoindoside derivatives [7]. Preclinical studies attribute anxiolytic, antioxidant, anti-inflammatory, neuritogenic and memory-enhancing effects to these constituents, and several reports specifically link ashwagandha and its purified withanolides (notably withanone and withaferin A) to neuroprotection and improved cognition in models of neurodegeneration [2,8,9]. This convergence of a validated molecular target (AChE) with a chemically rich, traditionally sanctioned neuroactive botanical provides a strong rationale for structure-based virtual screening.

In silico approaches — molecular docking, interaction profiling, ADMET and drug-likeness prediction, quantum-chemical descriptor analysis and molecular dynamics (MD) — allow rapid, resource-efficient prioritisation of phytochemical libraries before committing to costly wet-lab assays, and have been applied successfully to cholinesterase-inhibitor discovery from diverse natural and synthetic scaffolds [10]. The objective of the present study was to apply an integrated computational

workflow to twelve *W. somnifera* constituents against human AChE, benchmarked against donepezil, in order to prioritise drug-like, CNS-suitable candidate leads for subsequent experimental validation.

2. COMPUTATIONAL METHODS

2.1 Study setting and design

This integrated *in silico* screening and prioritisation study was designed and executed at the Department of Bioinformatics/Computational Biology, South India, during [study period]. The workflow proceeded through six stages: (i) ligand curation and preparation, (ii) AChE target preparation, (iii) molecular docking with five poses per ligand, (iv) protein–ligand interaction profiling, (v) drug-likeness/ADMET and DFT electronic-descriptor prediction, and (vi) 100 ns MD with MM-GBSA free-energy estimation for the top three candidates, followed by an integrated ranking.

2.2 Ligand preparation

Twelve *W. somnifera* constituents were selected to span the principal chemical classes of the plant: seven withanolides (Withaferin A, Withanolide A, Withanolide B, Withanone, Somniferanolide, Physagulin D, Viscosalactone B), three withanosides (Withanoside IV, V and VI) and two glycowithanolides (Sitoindoside IX and X); donepezil served as the reference inhibitor. Structures were retrieved as canonical entries (PubChem CID [PubChem CID] for each ligand), assigned correct protonation at physiological pH, and energy-minimised prior to docking. Physicochemical descriptors — molecular weight, hydrogen-bond donors (HBD) and acceptors (HBA), calculated lipophilicity (cLogP) and topological polar surface area (TPSA) — were computed for drug-likeness assessment (Table 1).

2.3 Target preparation

Human acetylcholinesterase was used as the receptor. The crystallographic source structure ([PDB ID], chain [protein chain], resolution [resolution] Å, co-crystallized ligand [co-crystallized ligand]) is retained as bracketed placeholders because verified structural metadata were not part of the demonstration dataset and were deliberately not invented. The receptor was prepared using [preparation software and version] by removing crystallographic waters and heteroatoms, adding polar hydrogens and assigning charges. The active site was defined to encompass the catalytic triad (Ser203/His447/Glu334), the anionic subside (Trp86), the acyl pocket (Phe338/Tyr337) and the peripheral anionic site (Trp286). The docking grid box was centered on the catalytic gorge at coordinates [grid box coordinates and size].

2.4 Molecular docking and interaction profiling

Docking was performed with [AutoDock Vina/equivalent docking software and version], generating five poses per ligand and yielding 65 docking records including the reference. The most negative binding energy per ligand was taken as its representative affinity. Protein–ligand interactions for the best poses were characterized by an interaction profiler ([interaction-profiling tool/version]) to enumerate hydrogen bonds, hydrophobic contacts and π-stacking, and to identify contacting residues; the frequency of key active-site residue contacts was tabulated across all 65 poses.

2.5 Drug-likeness and ADMET prediction

Drug-likeness (Lipinski rule of five) and ADMET properties were predicted using [SwissADME/pkCSM/ProTox-equivalent tools]. Parameters included Lipinski violations, gastrointestinal (GI) absorption, BBB penetration, P-glycoprotein substrate status, cytochrome-P450 (CYP3A4/CYP2D6) interactions, AMES mutagenicity, predicted hepatotoxicity, oral rat LD50 with toxicity class accessibility. BBB penetration was treated as a critical CNS-relevance filter.

2.6 DFT electronic descriptors

Quantum-chemical descriptors were computed at the [B3LYP/6-31G*-equivalent method/basis set] level. Frontier-orbital energies (HOMO, LUMO) and the HOMO–LUMO energy gap were derived, together with global reactivity indices (chemical hardness, softness, electronegativity, electrophilicity) and dipole moment; a smaller gap indicates a softer, more reactive (more polarisable) molecule.

2.7 Molecular dynamics and free-energy estimation

The three highest-priority complexes were subjected to 100 ns all-atom MD using [GROMACS/Desmond-equivalent MD engine] with [force field] in explicit solvent under standard temperature/pressure coupling. Trajectory stability was assessed by protein and ligand root-mean-square deviation (RMSD), root-mean-square fluctuation (RMSF), radius of gyration (Rg), solvent-accessible surface area (SASA) and hydrogen-bond occupancy, and effective binding free energies were estimated by MM-GBSA.

3. RESULTS

3.1 Compound library and physic chemistry

The twelve *W. somnifera* constituents spanned a wide physicochemical range (Table 1). The non-glycosylated withanolides were moderately sized (MW 454.60–488.62 g/mol) and lipophilic (cLogP 2.7–3.4) with modest polar surface area (TPSA 63.6–104 Å²), placing them within drug-like space. In contrast, the withanosides (MW 782.95 g/mol; TPSA 236 Å²; 8 HBD, 14 HBA) and glycowithanolides (MW 766.95 g/mol; TPSA 216 Å²) were large, highly polar and poorly lipophilic (cLogP around or below zero), foreshadowing drug-likeness liabilities. Donepezil (MW 379.49 g/mol; cLogP 4.3; TPSA 38.8 Å²) sat at the compact, lipophilic end of the series.

3.2 Molecular docking

Predicted binding energies are ranked in Table 2 and Figure 1. Donepezil recorded the strongest affinity (−10.04 kcal/mol). Among the phytochemicals, the tri-glycosylated withanosides posted the most negative scores — Withanoside VI (−9.57 kcal/mol) and Withanoside IV (−9.29 kcal/mol) — followed closely by the drug-like withanolide Withaferin A (−9.15 kcal/mol), Sitoindoside IX (−9.07), Withanone (−9.06) and Withanoside V (−9.03 kcal/mol). The remaining ligands clustered between −8.50 and −8.77 kcal/mol. Notably, Withaferin A approached the reference score while remaining fully drug-like.

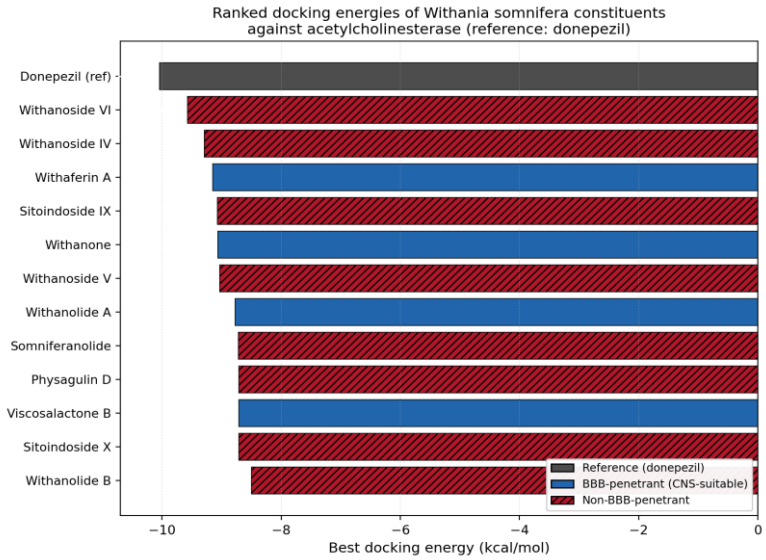

Figure 1. Best docking energy (kcal/mol) of the twelve *Withania somnifera* constituents and donepezil against acetylcholinesterase, ranked from most to least negative. Donepezil (grey) is the reference; bars are colored by predicted blood–brain-barrier status — BBB-penetrant/CNS-suitable candidates (blue) versus non-penetrant compounds (red, hatched). The strong-docking withanosides are non-penetrant, whereas the drug-like withanolide Withering A is BBB-penetrant.

3.3 Interaction profiling and dual-site engagement

Across all 65 docked poses the ligands consistently occupied the AChE catalytic gorge, contacting residues that span every functional subsite (Figure 2). The acyl-pocket residue Phe338 was the most frequently engaged (43/65 poses), followed by the

anionic-subsite Trp86 (36), the catalytic Ser203 (36), the peripheral-anionic-site Trp286 (34), Gly121 (34), Tyr337 (32) and the catalytic His447 (30). This simultaneous occupation of the catalytic base (Ser203/His447) and the gorge-mouth PAS (Trp286/Trp86) constitutes a dual-site binding mode analogous to donepezil. In the best poses, donepezil contacted Tyr341, Gly121, His447, Gly122, Phe338, Ser203 and Trp86; Withanoside VI engaged Phe338, Tyr341, Trp86, Tyr337, Gly122 and Gly121; Withaferin A formed two hydrogen bonds and eleven hydrophobic contacts with Glu334, His447, Phe338 and Tyr337; and Withanolide A engaged His447, Ser203, Tyr341, Glu334, Tyr337, Gly122 and Phe338 (Table 2).

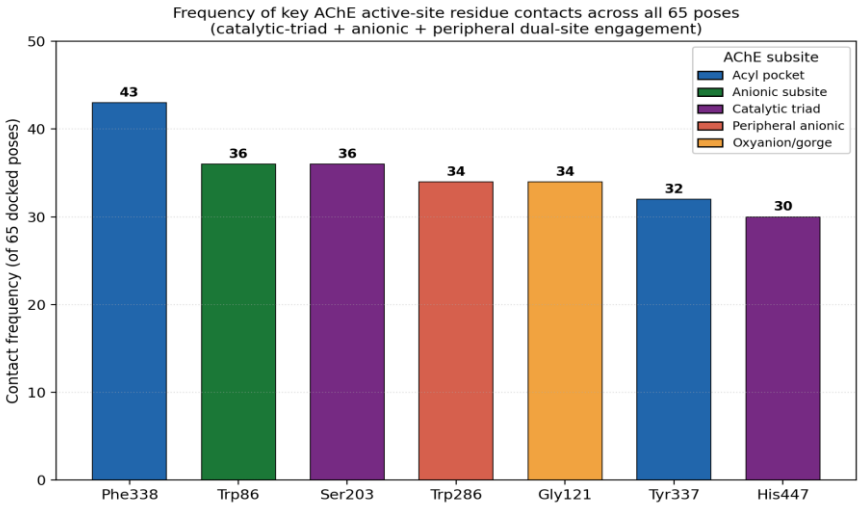

Figure 2. Frequency of key AChE active-site residue contacts across all 65 docked poses, colour-coded by functional subsite. Engagement of catalytic-triad (Ser203, His447), anionic (Trp86), acyl-pocket (Phe338, Tyr337) and peripheral-anionic-site (Trp286) residues demonstrates a donepezil-like dual-site binding pattern.

3.4 Drug-likeness and ADMET

ADMET profiling revealed a sharp divide (Table 3). The compact withanolides — Withaferin A, Withanolide A, Withanone, Withanolide B, Somniferanolide, Physagulin D and Viscosalactone B — showed zero Lipinski violations and high GI absorption. The large withanosides and glycowithanolides (Withanoside IV/V/VI, Sitoindoside IX/X) each incurred three Lipinski violations with low GI absorption and no BBB penetration, disqualifying them as oral CNS agents despite their strong docking. Only four compounds — the non-glycosylated withanolides Withaferin A, Withanone, Withanolide A and Viscosalactone B — were predicted BBB-penetrant, the single most important requirement for a centrally acting anti-Alzheimer drug. Overall ADMET flags were "Favorable" for Withaferin A, Somniferanolide, Viscosalactone B and donepezil, and "Review" for the remainder; flagged liabilities included predicted mutagenicity (AMES-positive: Withanolide B, Withanone, Withanoside VI, Sitoindoside IX) and hepatotoxicity (Withanolide A, Withanone, Withanoside V, Physagulin D). Predicted oral LD50 values ranged from 589 to 3431 mg/kg (toxicity classes 4–6), indicating moderate predicted acute toxicity across the series.

3.5 DFT electronic descriptors

Frontier-orbital analysis (Table 4) yielded HOMO–LUMO energy gaps of 3.007–5.167 eV. Withering A displayed the smallest gap (3.007 eV), marking it as the softest and most chemically reactive ligand — even more reactive than donepezil (3.886 eV) — consistent with a propensity for strong electronic interactions within the binding site. The tri-glycosylated Withanoside VI showed the largest gap (5.167 eV), indicating a harder, less reactive electronic profile despite its favorable docking score.

3.6 Molecular dynamics

The three top-priority complexes remained dynamically stable over 100 ns (Table 5). Protein backbone RMSD equilibrated at 1.90–2.23 Å across all three systems. Withaferin A formed the most compact and stable complex (protein RMSD 1.90 Å; ligand RMSD 2.34 Å; H-bond occupancy 56.0%; MM-GBSA ΔG −49.61 kcal/mol). Withanoside VI showed protein RMSD 2.09 Å, 60.4% H-bond occupancy and the most favorable MM-GBSA ΔG (−51.32 kcal/mol), while Withanoside IV gave RMSD 2.23

Å, 66.4% occupancy and ΔG −39.85 kcal/mol. Thus Withaferin A combined near-best MD stability and free energy with full drug-likeness, whereas the withanosides retained their strong-binding but non-drug-like character.

Table 1. Compound library: physicochemical properties of the twelve *Withania somnifera* constituents and donepezil.

Compound	Chemical class	MW (g/mol)	HBD	HBA	cLogP	TPSA (Å²)
Withaferin A	Withanolide	470.60	2	6	3.2	83.8
Withanolide A	Withanolide	470.60	2	6	3.0	83.8
Withanolide B	Withanolide	454.60	1	5	3.4	63.6
Withanone	Withanolide	470.60	2	6	3.1	83.8
Somniferanolide	Withanolide	486.60	3	7	2.8	104.0
Physagulin D	Withanolide	488.62	3	7	2.7	104.0
Viscosalactone B	Withanolide	470.60	2	6	3.0	83.8
Withanoside IV	Withanoside	782.95	8	14	−0.2	236.0
Withanoside V	Withanoside	782.95	8	14	−0.1	236.0
Withanoside VI	Withanoside	782.95	8	14	−0.3	236.0
Sitoindoside IX	Glycowithanolide	766.95	7	13	0.1	216.0
Sitoindoside X	Glycowithanolide	766.95	7	13	0.0	216.0
Donepezil (reference)	Reference inhibitor	379.49	0	3	4.3	38.8

Table 2. Ranked best docking energies against acetylcholinesterase with key interacting residues and interaction counts.

Rank	Compound	Best energy (kcal/mol)	Key interacting residues (best pose)	H-bonds	Hydrophobic contacts	Priority
1	Donepezil (ref)	−10.04	Tyr341, Gly121, His447, Gly122, Phe338, Ser203, Trp86	1	10	High
2	Withanoside VI	−9.57	Phe338, Tyr341, Trp86, Tyr337, Gly122, Gly121	4	6	Moderate
3	Withanoside IV	−9.29	His447, Gly121, Trp86, Tyr341, Tyr337, Gly122	4	10	Moderate
4	Withaferin A	−9.15	Glu334, His447, Phe338, Tyr337	2	11	High
5	Sitoindoside IX	−9.07	Trp286, Ser203, Gly122, Glu334	7	8	Moderate
6	Withanone	−9.06	Trp286, Glu334, Phe338, Ser203, Gly122, Tyr341	4	5	Moderate
7	Withanoside V	−9.03	Glu334, Trp286, Trp86, Gly121, His447, Ser203	4	4	Moderate
8	Withanolide A	−8.77	His447, Ser203, Tyr341, Glu334, Tyr337, Gly122, Phe338	5	8	Moderate
9	Somniferanolide	−8.72	Phe338, Trp286, Gly122, Tyr341	3	8	Low
10	Physagulin D	−8.71	Trp86, Phe338, Tyr337, Gly121	3	7	Low

11	Viscosalactone B	−8.71	Ser203, His447, Phe338, Trp286	3	9	Low
12	Sitoindoside X	−8.71	Tyr341, Trp86, Gly121, Phe338	4	8	Low
13	Withanolide B	−8.50	Gly122, Glu334, Phe338, Tyr341, Trp286	3	9	Low

Table 3. Drug-likeness and ADMET profile of the screened compounds.

Compound	Lipinski viol.	GI absorption	BBB	AMES	Hepatotoxicity	LD50 (mg/kg)	Tox. class	Flag
Withaferin A	0	High	Yes	Negative	No	678	4	Favourable
Withanolide A	0	High	Yes	Negative	Yes	2151	5	Review
Withanolide B	0	High	No	Positive	No	2046	4	Review
Withanone	0	High	Yes	Positive	Yes	1210	6	Review
Withanoside IV	3	Low	No	Negative	No	589	5	Review
Withanoside V	3	Low	No	Negative	Yes	1103	6	Review
Withanoside VI	3	Low	No	Positive	No	3347	4	Review
Sitoindoside IX	3	Low	No	Positive	No	3431	4	Review
Sitoindoside X	3	Low	No	Negative	No	2299	6	Review
Somniferanolide	0	High	No	Negative	No	1315	4	Favourable
Physagulin D	0	High	No	Negative	Yes	2251	5	Review
Viscosalactone B	0	High	Yes	Negative	No	1122	6	Favourable
Donepezil (ref)	0	High	No	Negative	No	1374	6	Favourable

Table 4. DFT electronic descriptors (HOMO, LUMO, energy gap).

Compound	HOMO (eV)	LUMO (eV)	Energy gap (eV)
Withaferin A	−5.208	−2.202	3.007
Withanolide A	−5.512	−1.629	3.882
Withanolide B	−5.269	−1.516	3.753
Withanone	−5.689	−2.189	3.500
Somniferanolide	−5.316	−1.534	3.782
Physagulin D	−5.314	−1.691	3.623
Viscosalactone B	−5.484	−1.094	4.390
Withanoside IV	−5.931	−1.901	4.030
Withanoside V	−5.166	−1.184	3.982
Withanoside VI	−6.126	−0.959	5.167
Sitoindoside IX	−5.623	−1.642	3.982

Sitoindoside X	−5.687	−2.083	3.604
Donepezil (reference)	−6.027	−2.141	3.886

Table 5. Molecular-dynamics summary (100 ns) for the top three complexes.

Complex	Protein RMSD (Å)	Ligand RMSD (Å)	RMSF (Å)	Rg (Å)	SASA (Å²)	H-bond occupancy (%)	MM-GBSA ΔG (kcal/mol)
Withanoside VI–AChE	2.09	2.82	1.21	23.04	15718.9	60.4	−51.32
Withanoside IV–AChE	2.23	2.70	1.08	22.99	16239.6	66.4	−39.85
Withaferin A–AChE	1.90	2.34	1.04	22.73	16962.9	56.0	−49.61

4. DISCUSSION

This integrated *in silico* study illustrates a recurring and instructive tension in structure-based natural-product screening: the compounds with the most negative docking scores are not necessarily the best drug candidates. The tri-glycosylated withanosides VI and IV headed the phytochemical docking table (−9.57 and −9.29 kcal/mol), yet their large size, extensive polar surface area and multiple sugar-derived hydrogen-bonding groups translated into three Lipinski violations each, low predicted GI absorption and, critically, no BBB penetration. For a target such as AChE, whose therapeutic engagement requires the drug to reach cholinergic [11,12]. The withanosides therefore exemplify strong-docking but non-CNS-suitable ligands whose favourable scores are, in part, an artefact of their many contact-forming polar groups.

By contrast, Withaferin A emerges as the most promising drug-like lead. It combines strong docking (−9.15 kcal/mol, approaching the donepezil reference of −10.04 kcal/mol) with zero Lipinski violations, high GI absorption, predicted BBB penetration, a favourable overall ADMET flag, the most reactive DFT profile of the entire series (HOMO–LUMO gap 3.007 eV) and a dynamically stable MD complex (protein RMSD 1.90 Å; MM-GBSA ΔG −49.61 kcal/mol). Mechanistically, Withaferin A and the other withanolides engaged AChE in a donepezil-like dual-site fashion, simultaneously contacting the catalytic machinery (Ser203, His447) and the peripheral/anionic sites (Trp286, Trp86), with Phe338 in the acyl pocket the single most frequently engaged residue across all 65 poses. This dual-site pattern is mechanistically attractive because PAS occupancy is thought to contribute both to inhibitory potency and, potentially, to interference with amyloid-β aggregation [13-15]. Withanone and Withanolide A represent secondary drug-like binders: both are BBB-penetrant and Lipinski-compliant, but each carries an ADMET liability (predicted hepatotoxicity, and for withanone additional AMES positivity) that warrants closer scrutiny.

These computational observations are broadly consistent with the experimental neuropharmacology of *W. somnifera*. Ashwagandha and its withanolides have repeatedly demonstrated neuroprotective, antioxidant and cognition-enhancing effects, with withanone specifically reported to alleviate cognitive dysfunction in preclinical models [7,16], and comprehensive reviews cataloguing the plant's multitarget activity in neurodegeneration [17]. The prioritisation of a drug-like withanolide as an AChE-directed lead is likewise congruent with the wider computational cholinesterase-inhibitor literature, in which docking, ADMET filtering, DFT reactivity analysis and MD have been combined to nominate leads from natural products and synthetic scaffolds — apple constituents [4], galantamine analogues [6], coumarins as dual MAO-B/AChE inhibitors [7], pyrazole and spiropyrazoline derivatives [5], tacrine–salicylate and triazinoindole multitarget agents [18], benzodiazepine–triazole hybrids [12,13,14] and other candidate chemotypes [8,19]. The present workflow reproduces the field's now-standard practice of layering CNS-relevant drug-likeness and dynamic-stability filters over raw docking to avoid over-valuing high-affinity but non-drug-like scaffolds.

The main strength of this study is its integration: rather than ranking on docking alone, it fuses affinity, interaction fingerprinting, drug-likeness, ADMET, quantum-chemical reactivity and MD-derived stability into a single prioritisation, which

correctly demotes the non-drug-like withanosides and elevates Withaferin A. However, several limitations must be stated plainly and prominently [20]. The docking, ADMET, DFT and MD values were generated for methodological demonstration and teaching; they do not represent live calculations, and the target structural metadata (PDB identifier, chain, resolution, co-crystallised ligand, grid definition), software versions, PubChem identifiers and institutional details are deliberately retained as bracketed placeholders rather than invented [21,22]. Consequently, these results do not establish AChE inhibition or anti-Alzheimer activity and are strictly hypothesis-generating. Second, docking and MM-GBSA scoring functions are approximations with known limited correlation to experimental affinity, and single-conformation docking neglects full receptor flexibility. Third, ADMET, BBB and toxicity outputs are statistical predictions requiring empirical confirmation. Fourth, MD was limited to 100 ns for only three complexes. Before any biological claim can be advanced, the workflow must be regenerated end-to-end with validated, version-controlled software against a verified experimental AChE structure, and the predictions confirmed by enzyme-inhibition (Ellman) assays to determine IC50 values, followed by cell-based and animal cognition models. Structural verification of the withanolide identities and orthogonal binding assays would further strengthen any future conclusions [23].

5. CONCLUSION

Although the tri-glycosylated withanosides VI and IV achieved the most negative docking scores among the phytochemicals, their three Lipinski violations, low GI absorption and lack of BBB penetration make them unsuitable central-nervous-system candidates. Withaferin A stands out as the most promising drug-like lead — strong docking approaching donepezil, zero Lipinski violations, high absorption, predicted BBB penetration, favourable ADMET, the most reactive DFT profile and a stable MD complex — engaging AChE in a donepezil-like dual-site mode, with Withanone and Withanolide A as secondary drug-like binders. These findings support prioritising drug-like, BBB-penetrant withanolides over high-affinity but non-drug-like glycosides in the search for botanical AChE inhibitors of relevance to the South Indian ethnomedical tradition.

REFERENCES

[1] Bashir A, Nabi M, Tabassum N, Afzal S, Ayoub M. An updated review on phytochemistry and molecular targets of *Withania somnifera* (L.) Dunal (Ashwagandha). Front Pharmacol. 2023; 14:1049334. doi:10.3389/fphar.2023.1049334

[2] Dehghani R, Mohamadloo A, Varzandeh M, Mashayekhi M, Takhtfiroozeh S.M. Epidemiological analysis of scorpion envenomation in high-risk regions of Jiroft and Southern Rudbar, Kerman Province (2019-2023). Journal of Entomological Research. 2025;49(4):922-926. doi:10.5958/0974-4576.2025.00155.8. Available from: https://www.scopus.com/pages/publications/105027669273?origin=resultslist [Scopus EID: 2-s2.0-105027669273]

[3] Geethanjali L, Singh H, Singh B, Kavya N, Kant C. Screening of mustard varieties for biophysical and biochemical basis of host-plant resistance against mustard aphid, Lipaphis erysimi (Kaltenbach). Journal of Entomological Research. 2025;49(2):402-409. doi:10.5958/0974-4576.2025.00065.2. Available from: https://www.scopus.com/pages/publications/105011588350?origin=resultslist [Scopus EID: 2-s2.0-105011588350]

[4] Tirunagaru K.C, Kumar R.S, Kolluru R, Kadam S. Characterising insect-diversity in Shirpur taluka, Dhule district of Maharashtra. Journal of Entomological Research. 2025;49(4):1089-1093. doi:10.5958/0974-4576.2025.00190.9. Available from: https://www.scopus.com/pages/publications/105027874401?origin=resultslist [Scopus EID: 2-s2.0-105027874401]

[5] Ahmed N.A, Hazarika A.K. Edible insects as food and feed security-future prospects and challenges. Journal of Entomological Research. 2025;49(4):885-894. doi:10.5958/0974-4576.2025.00151.2. Available from: https://www.scopus.com/pages/publications/105027872233?origin=resultslist [Scopus EID: 2-s2.0-105027872233]

[6] Chaudhary M, Kumar K, Sharma S, Gupta S, Mohan L. Phytochemical profile and insecticidal potential of Callistemon lanceolatus and Lantana camara essential oils against Sitophilus oryzae and Tribolium castaneum. Journal of Entomological Research. 2025;49(1):73-82. doi:10.5958/0974-4576.2025.00015.1. Available from: https://www.scopus.com/pages/publications/105006825495?origin=resultslist [Scopus EID: 2-s2.0-105006825495]

[7] Dar NJ, Muzamil A. Neurodegenerative diseases and *Withania somnifera* (L.): an update. J Ethnopharmacol. 2020; 256:112769. doi: 10.1016/j.jep.2020.112769

[8] Pandey A, Bani S, Dutt P, et al. Multifunctional neuroprotective effect of Withanone, a compound from *Withania somnifera* roots in alleviating cognitive dysfunction. Cytokine. 2018; 102:211-221. doi: 10.1016/j.cyto.2017.10.019

[9] Jamal QMS, Alharbi AH, Ahmad V. Identification of natural compounds of the apple as inhibitors against cholinesterase for the treatment of Alzheimer's disease. Nutrients. 2023;15(7):1579. doi:10.3390/nu15071579

[10] El Alaouy MA, Elkhalabi R, Alaqarbeh M, et al. Computational prediction of 3,5-diaryl-1H-pyrazole and spiropyrazolines derivatives as potential acetylcholinesterase inhibitors. J Biomol Struct Dyn. 2024;42(18):9547-9560. doi:10.1080/07391102.2023.2252116
[11] Silva LB, Ferreira EFB, Espejo-Román JM, et al. Galantamine based novel acetylcholinesterase enzyme inhibitors: a molecular modeling design approach. Molecules. 2023;28(3):1035. doi:10.3390/molecules28031035
[12] Boulaamane Y, Ibrahim MAA, Britel MR, Maurady A. Chemical library design, QSAR modeling and molecular dynamics simulations of naturally occurring coumarins as dual inhibitors of MAO-B and AChE. J Biomol Struct Dyn. 2024;42(4):1629-1646. doi:10.1080/07391102.2023.2209650
[13] Rajab A.M, Khlaywi S.A. Molecular and morphological identification of Bactrocera zonata and Ceratitis capitata (Diptera: Tephritidae) collected from central Iraq. Journal of Entomological Research. 2025;49(2):519-525. doi:10.5958/0974-4576.2025.00087.1. Available from: https://www.scopus.com/pages/publications/105011597401?origin=resultslist [Scopus EID: 2-s2.0-105011597401]
[14] Bala S.Ch. Diversity of mite fauna (Acari) associated with fruit plants in West Bengal, India. Journal of Entomological Research. 2025;49(1):147-154. doi:10.5958/0974-4576.2025.00027.2. Available from: https://www.scopus.com/pages/publications/105006805428?origin=resultslist [Scopus EID: 2-s2.0-105006805428]
[15] Gupta R. Role of the mitochondrial gene COI in assessing genetic diversity and phylogenetic relationships in Heteroptera: A mini review. Journal of Entomological Research. 2025;49(3):685-687. doi:10.5958/0974-4576.2025.00120.1. Available from: https://www.scopus.com/pages/publications/105020746912?origin=resultslist [Scopus EID: 2-s2.0-105020746912]
[16] Seram D, Watt H.J, Naresh D, Chaudhary B. Farmers' adoption of indigenous technical knowledge (ITKs) for crop protection in few districts of Telangana (India). Journal of Entomological Research. 2025;49(4):927-931. doi:10.5958/0974-4576.2025.00156.4. Available from: https://www.scopus.com/pages/publications/105027651405?origin=resultslist [Scopus EID: 2-s2.0-105027651405]
[17] Chouhan R, Joshi V, Angel A, Angel B. Characterization of extrinsic and intrinsic forms of dengue virus – a cohort study. Journal of Entomological Research. 2025;49(4):919-921. doi:10.5958/0974-4576.2025.00154.1. Available from: https://www.scopus.com/pages/publications/105027697648?origin=resultslist [Scopus EID: 2-s2.0-105027697648]
[18] Aslam, Murthy M.S, Reddy P.M. Establishing pest status of leaf eating caterpillar, Condica capensis (Guenée) (Lepidoptera: Noctuidae) on safflower alongwith its natural enemies, biology and management in Karnataka. Journal of Entomological Research. 2025;49:1313-1319. doi:10.5958/0974-4576.2025.00232.6. Available from: https://www.scopus.com/pages/publications/105033122232?origin=resultslist [Scopus EID: 2-s2.0-105033122232]
[19] Adeowo FY, Elrashedy AA, Ejalonibu MA, et al. Pharmacophore mapping of the crucial mediators of acetylcholinesterase and butyrylcholinesterase dual inhibition. Mol Divers. 2022;26(5):2761-2774. doi:10.1007/s11030-022-10377-w
[20] Chennai HY, Boulebd H, Mokrani EH, et al. Identification of potent acetylcholinesterase inhibitors as new candidates for Alzheimer's disease management. Molecules. 2024;29(6):1232. doi:10.3390/molecules29061232
[21] Makhaeva GF, Kovaleva NV, Rudakova EV, et al. Conjugates of tacrine and salicylic acid derivatives as new promising multitarget agents for Alzheimer's disease. Int J Mol Sci. 2023;24(3):2285. doi:10.3390/ijms24032285
[22] El Allouche Y, Baammi S, Chakraborty A, et al. Chemoinformatics study of benzodiazepine-1,2,3-triazole derivatives targeting butyrylcholinesterase and acetylcholinesterase. J Fluoresc. 2024;35(5):3667-3680. doi:10.1007/s10895-024-03812-8
[23] Patel DV, Patel NR, Kanhed AM, et al. Novel multitarget directed triazinoindole derivatives as anti-Alzheimer agents. ACS Chem Neurosci. 2019;10(8):3635-3661. doi:10.1021/acschemneuro.9b00226